

# Experimental and FEM Research on Drop Tests of Electronic Devices

Li Xingzhou, Zhang Guoqiang, Dong Daokun

The Department of Packaging Engineering, Shandong University Jinan, China

**Abstract:** The ability of electronic devices, such as personal digital assistants and digital cameras, to withstand accidental impacts and shock is essential. In this paper, two research methods on a whole-packaged scanner's ability of shock are employed. One is the experimental test in accordance with GB/T4857.5-92 about transport packages-vertical impact test method by dropping. During the test, the data acquisition device obtains useful data from strain gauges and acceleration sensors. To avoid the disadvantages of the experimental method, the finite element method is also conducted. An advanced analytical simulation for the various drop orientations is performed to evaluate the structural performance of the product and demonstrate their compliance with regulatory requirements. Comparisons show good correlation between experimental and finite element methods. In addition, this paper intends to provide some guidance on the research of packaging performance of electronic products.

**Keywords:** finite element method; modeling and simulation; drop test; cushion package

## 1. Introduction

In recent years, rapid developments in the electronic information industry have brought large numbers of electronic and information products like personal digital assistants, mobile phones and digital cameras to our daily life [1]. The most common damage to these devices comes from accidental drop onto hard ground due to rough delivery and usage.

Traditionally, physical drop tests are performed on prototypes to ensure the products packaging quality and reliability. Generally, these tests are qualitative. However, once the product is equipped with strain gauges and acceleration sensors, the needful data, such as strain and acceleration at some interested points during the impact, can be acquired via data acquisition device. While physical tests may provide the most direct and accurate results for evaluating the packaging property, the experimental drop test is expensive, time consuming and require extensive effort.

Considering the disadvantage of the experimental method, the numerical simulation is applied to investigate the packaging property of the electronic devices. Now, as the rapid improvement of hardware and the finite element software, the simulation-based virtual test for complex electronic devices has become available and easy accessible [2]. In this paper, the elapsed time necessary to run an analysis is sharply shortened because of the finite element software supporting shared memory parallel processing or the massively parallel processing capabilities and automatically identifying the contact conditions of the assembly of the electronic product.

## 2. Finite Element Model

### 2.1. Real Scanner Description and Geometry Simplification

The real scanner in this paper is mainly composed of

upper housing, middle housing with platen glass, scanning head, PCB plate, data interface, stepper motor and bottom housing. In order to avoid the solution fails to converge and shorten the elapsed time necessary to run an analysis, some simplifications, such as small holes and some round comers, should be considered. However, the supporting and connection structures must be described as detailed as possible, because the force between different components is passed by these areas.

### 2.2. Finite Element Mesh

The whole geometric model of the scanner packages consists of the corrugated paper box, crushable foam and the scanner. The assembly modeling totally includes twenty-one different parts. As the finite element mesh is the key factor for the analysis time and the accuracy, the 3D geometric model must be meshed properly. As much as hexahedron elements should be used, so the "Hex Dominant" is chosen for mesh method and the "Quad/Tri" is defined for the free face mesh type in order to successfully mesh all parts, especially for some free-form surfaces. Fig. 1 shows the finite element mesh for the whole packaged scanner and some meshing details. For the connection area between different parts, finer mesh should be used to avoid converge problems and get authentic results as shown in Fig. 2. and Fig. 3.

### 2.2. Material Constitutive Models

The material constitutive models play an important role in the finite element simulation. It is important to consider the material properties, especially when modeling impact problems are the strain rate effect and plasticity. Materials behave differently under different regimes of strain rate. Many materials are found to be rate sensitive and there is a need to reflect this phenomenon correctly

in the analysis in order to obtain accurate results. Therefore, the material data used by any finite element model must be appropriate for the range of strain rates and strains experienced by the model during the simulation. Otherwise, significant errors may occur [3].

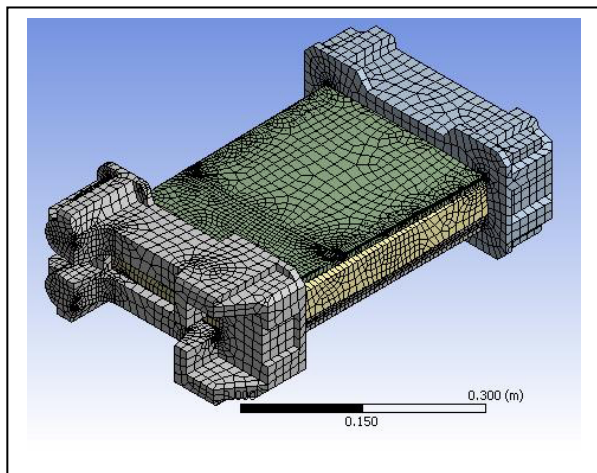


Figure 1. Overview of the inside finite element

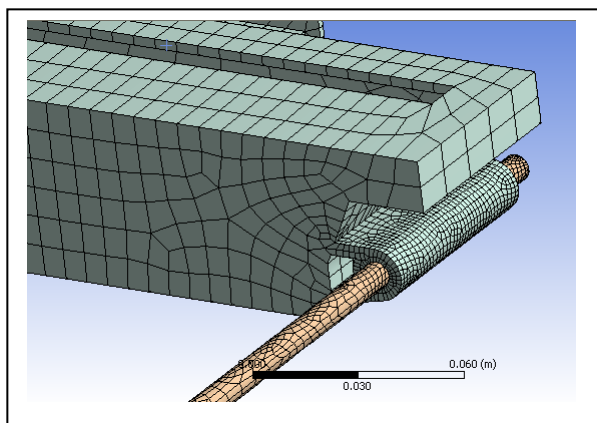


Figure 2. Mesh details of the connection area between scanning head and sliding rod

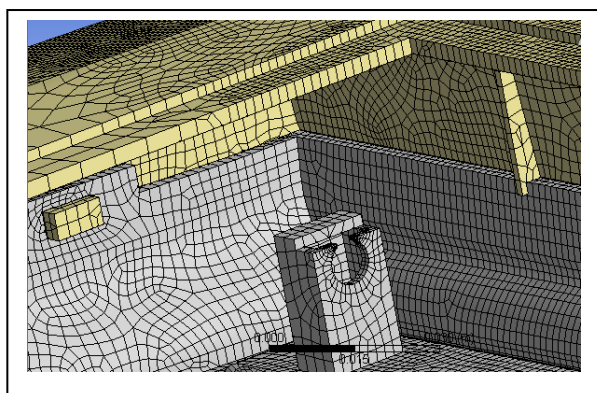


Figure 3. Mesh details of the connection area between middle housing and bottom housing

In this paper, the material models are generally defined by the following parameters: density, Young's modulus, plasticity and strain rates. Some material models used in this paper are just chosen from the material library of the analysis software [4]. But for a number of material models, material data obtained from experimental tests are converted into the format required by the program. Materials used in the simulation of this paper are listed in Table 1.

Table 1. Material Properties

Component Part	Material	Material Properties				
		DENS (kg/m <sup>3</sup> )	EX (Pa)	NUXY	Yield Stress (Pa)	Tangent Modulus (Pa)
housing	ABS	$1.04 \times 10^3$	$2.05 \times 10^9$	0.4	$2.303 \times 10^7$	$9 \times 10^8$
scanning head	PC	$1.2 \times 10^3$	$2.2 \times 10^9$	0.38	$6 \times 10^7$	$8 \times 10^8$
sliding rod	Steel	$7.9 \times 10^3$	$2.1 \times 10^{11}$	0.3	-	-
platen glass	Plexiglass	$2.5 \times 10^3$	$6 \times 10^{10}$	0.25	-	-
box	Corrugated cardboard	$1.5 \times 10^3$	$2.5 \times 10^9$	0.32	-	-
PCB plate	Composite material	$2.4 \times 10^3$	$2 \times 10^{10}$	0.35	-	-
target ground	Steel	$7.58 \times 10^3$	$2.07 \times 10^{11}$	0.3	-	-
buffering cushion	EPS	12	$1.45 \times 10^6$	-	-	-

Crushable foam is widely used in cushion packaging. Its mechanical behavior is sensitive to the strain rate, and this effect can be introduced by a piecewise linear law or by the overstress power law model. The compression-strain curve for the foam used in this paper is shown in Fig. 4.

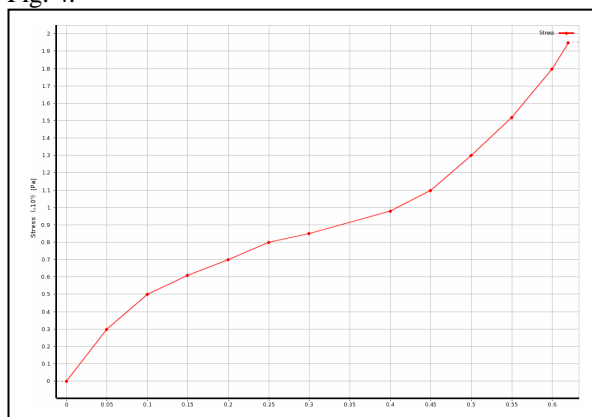


Figure 4. Foam compression strain diagram

### 2.3. Outline of Analysis Setting

When the three-dimensional (3D) geometric mode built in Pro/Engineer is imported into the analysis software, connections between different components are automatically identified and established as shown in. But these connections are all "Bonded" and not all appropriate to the practical situation, some manner settings must

be made in order to get authentic simulations.

There are five connection types we can choose from the drop-down box, Bonded, No separation, Frictionless, Rough, Frictional. The differences in the contact settings determine how the contacting bodies can move relative to one another. Depending on the type of problem to solve in the paper, just the Bonded and Fictional are applied to contact regions.

In order to reduce the analysis time for the scanner drop simulation, the whole packaged model is given an initial velocity of 3.9679m/s equaling to that obtained when dropped from the desired drop height, perpendicular to the target ground, instead of simulating the scanner dropping from its drop height. Besides, the “On Geometric Strain Limit” should be turned off and the “Step Controls” must be set properly.

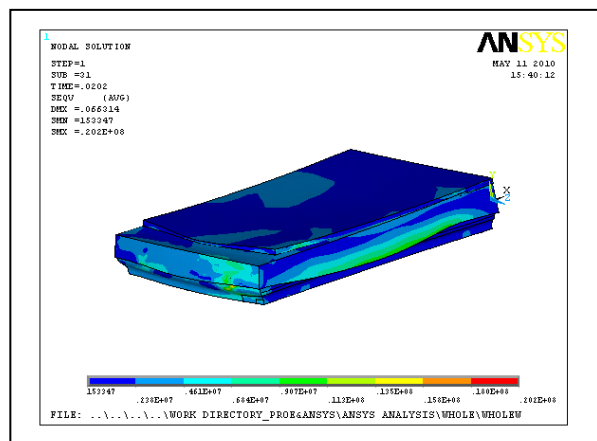


Figure 5. The distribution of equivalent elastic strain of bottom-down drop

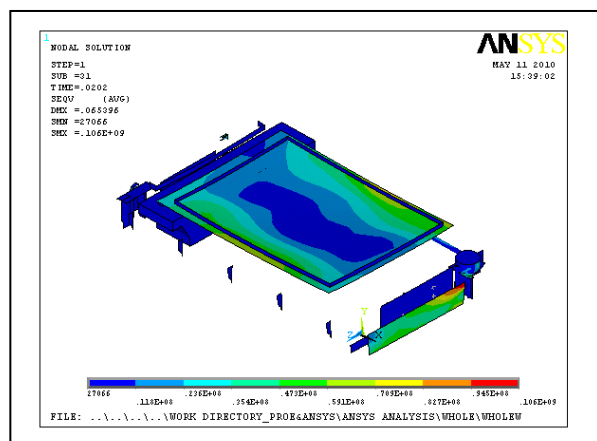


Figure 6. The details of equivalent elastic strain of bottom-down drop

### 3. Simulation Results

In the paper, five different drop cases defined by different drop orientations are simulated to thoroughly investigate the shock resistance of the whole packaged elec-

tronic device. They are bottom-down drop, short-side drop, long-side drop, short-side-edge drop, long-side-edge drop and short-side-corner drop. For each case, analytical results can be reported and discussed in term of total deformation, total and directional velocity, total and directional acceleration, equivalent elastic strain, equivalent stress, energy summary, contact force etc. In this paper, there is not enough space to list every result term for each case, so some results will be chosen to be discussed as an example in what follows.

#### 3.1. Equivalent Elastic Strain

The distribution of equivalent elastic strain of bottom-down drop is shown as Fig. 5 and Fig. 6. For the middle housing and bottom housing, the long sides suffer bigger elastic strain than the other regions. At the main contact regions, such as the bayonet coupling and coupling screws between middle and bottom housings, the stress concentration is remarkable. Besides, the contour indicates the PCB plate, scanning head and stepper motor are easily damaged during the impact. For the whole packaged device, the Maximum elastic strain occurs at the top left corner of the data interface.

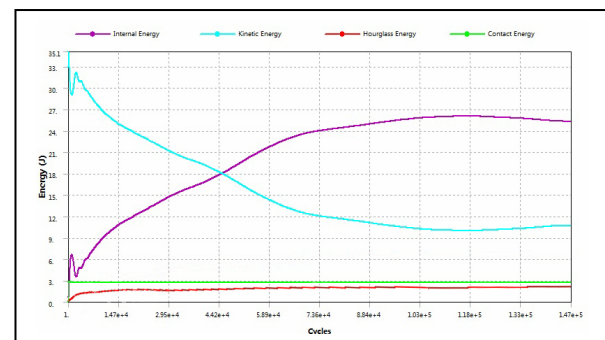


Figure 7. Energy summary

#### 3.2. Energy Summary

The Energy Summary shows plot of internal energy, kinetic energy, hourglass energy and contact energy as shown in Fig. 7. More attention should be paid to hourglass energy. When performing an explicit dynamics analysis with reduced integration elements, it is always important to determine whether hourglass effects have significantly degraded the results. As a general guideline, the hourglass energy should not exceed 10% of the internal energy. The hourglass energy can be compared to the internal energy by reviewing [5]. Besides, the curve clearly shows the energy conversion between internal energy and kinetic energy as the shock processing.

#### 3.3. Acceleration

Fig. 8 shows the distribution of total acceleration for short-side-corner drop at the time 0.0152s after the impact occurs. The contour clearly illuminates that the foam

suffers much more impact acceleration than the scanner and the impact acceleration of the scanner is generally inversely proportional to the distance between concerned points to impact point.

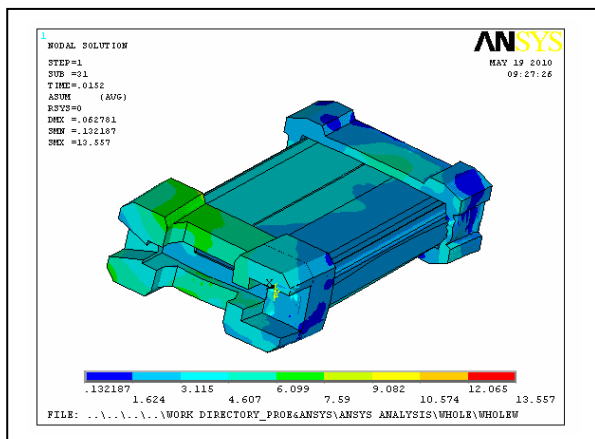


Figure 8. Distribution of total acceleration

## 4. Experimental Test

### 4.1. Test Aim and Arrangement

The targets of the actual drop test using the real scanner are to verify the reliability of numerical tools and modeling methodology adopted in this paper. According to the procedures illustrated in GB/T4857.5-92 about transport packages-vertical impact test method by dropping, five different groups of dropping test including three different faces drop, one edge and one corner drop are conducted. The test equipment mainly consists of the drop test machinery, data acquisition devices, data recording devices and the sensor as shown in Fig. 9.

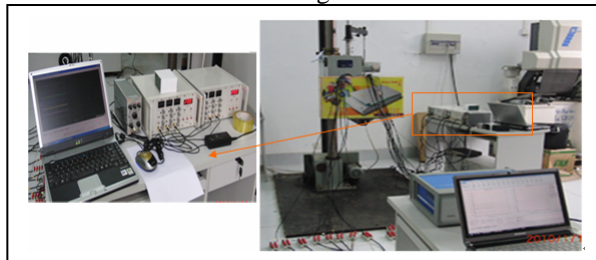


Figure 9. Test equipment

Before the test, ten strain gauges and three acceleration sensors are equipped at concerned regions. Detailed information of these sensors can be found in Table 2 and Table 3. Besides, more intuitionistic details are shown as Fig. 10 and Fig. 11. For the experiment, a set of three impact drops is performed for each impact orientation.

### 4.2. Comparison of the two Methods

The variations of the strain and acceleration at the certain regions during the impacting can be recorded by the

computer. These useful data are compared to numerical simulation results now.

Table 2. The Location of Strain Gauges

Location	Details		
	Direction	Number	Type
sliding rod	X	1	strain gauge 01
data interface	Y	2	strain rosette 01
data interface	Z	3	strain rosette 01
PCB	Y	4	strain rosette 02
PCB	Z	5	strain rosette 02
bottom housing	X	6	strain gauge 02
middle housing	Z	7	strain rosette 03
middle housing	45°	8	strain rosette 03
middle housing	X	9	strain rosette 03
platen glass	X	10	strain rosette 04
platen glass	Z	11	strain rosette 04
middle housing	X	12	strain rosette 05
middle housing	Z	13	strain rosette 05
right-middle housing	X	14	strain gauge 03
front-middle housing	Z	15	strain gauge 04
upper housing	X	16	strain guage 05

Table 3. The Location of Acceleration Sensors

Sensor	Details		
	Location	Direction	Number
1 (three-D)	Foam	Z	1
1 (three-D)	Foam	X	2
1 (three-D)	Foam	Y	3
2 (three-D)	Left of scanner	Z	4
2 (three-D)	Left of scanner	X	5
2 (three-D)	Left of scanner	Y	6
3 (single-dimensional)	Bottom of scanner	Z	7

1) *Comparison of Strain:* The time-strain curve of bottom-down drop is shown as Fig. 12. The maximum strain of channel 4,5,6,7,10,12,13 is obviously bigger than other channels. According to Table.2, this is generally consonant with the simulation result as shown in Fig. 6.

2) *Comparison of Acceleration:* The time-acceleration curve of short-side-corner drop is shown as Fig. 13. The maximum acceleration of the channel 1, 2, 3 is more than other channels. According to table.3, this implies that the foam suffers more impact and this





Figure 10. The location of strain gauges

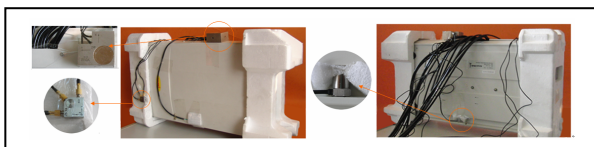


Figure 11. The location of acceleration sensors

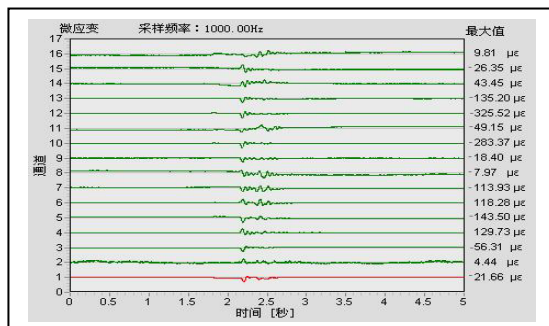


Figure 12. Time-strain curve of bottom-down drop

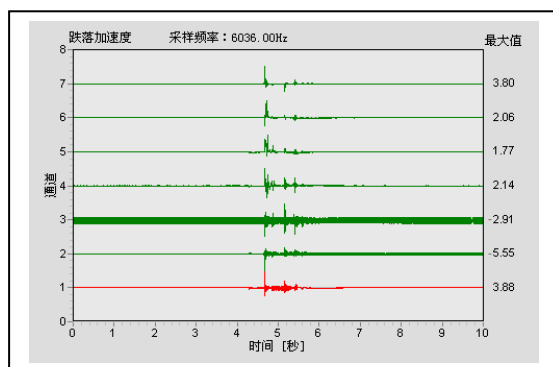


Figure 13. Time-acceleration curve of bottom-down drop

3) corresponds well with Fig. 8. Besides, the total acceleration of sensor 2 can be calculated:  $a_{\text{total}} =$

$(2.14^2 + 1.77^2 + 2.06^2)^{1/2} = 3.46g$ . While the simulation result getting from the Fig. 13 is between 3.115g and 4.607g, so the results abstained from the two methods are very close.

The comparisons for other drop cases are similar to the above cases. Although the results abstained from different ways are not fully consistent, they generally correspond well.

## Conclusion

In this study, an advanced analytical simulation of the drop impact of a whole packaged scanner was performed. The shock resistance of the whole packaged electronic device can be easily and totally studied from the result of simulation. Also, actual drop tests using a real scanner were carried out to verify the analysis results by comparing the strain and acceleration at some certain regions.

In general, the numerical simulation results correspond well with the experimental test results. Results obtained from both analytical simulation and experiment show that the PBC, platen glass and the contact regions between middle and bottom housings tend to be easily damaged during the drop impact. Besides, the acceleration got from the both two methods also basically corresponds well. The correlation between the simulation and experiment demonstrates that the numerical simulation method is reliable in investigating the impact properties of electronic device packing. So this numerical method can also be extended to other electronic devices such as mobile telephones, portable computers and digital cameras. And this numerical method can also be used in the new product designing to reduce product development cycles.

## References

- [1] Kap-Sun Kima, Sung-Hwan Chung, Jong-Soo Kim, Kyu-Sup Choi, Hyun-Do Yun, "Demonstration of structural performance of IP-2 packages by advanced analytical simulation and full-scale drop test," Nuclear Engineering and Design, vol. 240, Issue 3, pp. 639-655 March 2010.
- [2] Y.Y.Wang, C.Lu, J.Li, X.M.Tan, Y.C.Tse, "Simulation of drop/impact reliability for electronic devices," Finite Elements in Analysis and Design, Vol.41, 2005.
- [3] Chwee-Teck Lim, Y.M.Teo, V.P.W.Shim, "Numerical simulation of the drop impact response of a portable electronic product," Components and Packaging Technologies, vol. 25, Issue 3, pp. 478-485 September 2002.
- [4] Seungho Lim, Kyungtae Kim, Chanho Choi, No-Cheol Park, Young-Pil Park, Kyoung-Su Park, Ik-Joo Cha, "Finite-Element Shock Analysis of Slim Optical Disk Drives," IEEE Transactions on Magnetics, vol. 45, Issue 5, pp. 2213-2216, May 2009.
- [5] ANSYS, Inc, Mechanical APDL Documentation Descriptions, Release 12.1 - © 2009 SAS IP, Inc